INL/CON-08-14623
PREPRINT

# A Preliminary Assessment of Beryllium Dust Oxidation During a Wet Bypass Accident in a Fusion Reactor

## 25th Symposium on Fusion Technology

Brad J. Merrill
Richard L. Moore
J. Phillip Sharpe

September 2008

The INL is a
U.S. Department of Energy
National Laboratory
operated by
Battelle Energy Alliance

# A preliminary assessment of beryllium dust oxidation during a wet bypass accident in a fusion reactor

Brad J. Merrill, Richard L. Moore, J. Phillip Sharpe

Idaho National Laboratory, Idaho Falls, ID, USA

E-mail: Brad.Merrill@inl.gov

**Abstract**

A beryllium dust oxidation model has been developed at the Idaho National Laboratory (INL) by the Fusion Safety Program (FSP) for the MELCOR safety computer code. The purpose of this model is to investigate hydrogen production from beryllium dust layers on hot surfaces inside a fusion reactor vacuum vessel (VV) during in-vessel loss-of-cooling accidents (LOCAs). This beryllium dust oxidation model accounts for the diffusion of steam into a beryllium dust layer, the oxidation of the dust particles inside this layer based on the beryllium-steam oxidation equations developed at the INL, and the effective thermal conductivity of this beryllium dust layer. This paper details this oxidation model and presents the results of the application of this model to a wet bypass accident scenario in the ITER device.

**Keyword:** Fusion safety, beryllium dust oxidation, wet bypass accident, ITER

## 1. Introduction

As part of an ITER Implementing Task Agreement (ITA) between the ITER US Participant Team (PT) and the ITER International Team (IT), a beryllium dust oxidation model has been developed at the Idaho National Laboratory (INL) by the Fusion Safety Program (FSP) for the MELCOR 1.8.5 [1] fusion safety analysis computer code [2]. The purpose of this model is to investigate hydrogen production from beryllium dust layers on hot surfaces inside a fusion reactor vacuum vessel (VV) during in-vessel loss-of-cooling accidents (LOCAs). The accident of concern is a LOCA that produces a relatively slow VV pressurization event; that is, a LOCA that will not re-suspend the beryllium dust that has been deposited in groves between first wall (FW) tiles, but rapid enough to provide the required steam pressure for the reaction to proceed while the dust is still hot. This beryllium dust oxidation model accounts for the diffusion of steam into a beryllium dust layer, the oxidation of the dust particles inside this layer based on the beryllium-steam oxidation equations developed at the INL, and the effective thermal conductivity of this beryllium dust layer. We performed a parametric heat transfer study

with this model to investigate the possibility of a complete oxidation of beryllium dust in the grooves between first wall (FW) tiles of the ITER device during a wet bypass accident.

The following sections of this article present the physical components of this dust layer oxidation model which are: dust layer oxidation, effective thermal conductivity, and gap conductance heat transfer. Section 3 describes the application of this model to analyzing the beryllium dust layer in the grooves between first wall (FW) tiles of the ITER device during a wet bypass accident. In the final section, we summarize our findings.

**2. Dust layer model**

The oxidation of some materials has been experimentally demonstrated to proceed in three distinct oxidation regimes [3]. This appears to be the case for beryllium as can be seen in Figure 1, which contains a log plot of experimentally derived oxidation rate equations (kg-Be/$m^2$-s) as a function of inverse temperature (1/K) for fully dense (98%) beryllium [4]. The reaction kinetics in Regime I, a low temperature regime, are limited by the reactivity of the base metal, which proceeds at a much slower rate than inter-pore diffusion of the steam into the bulk of the base material. At very high temperatures, Regime III, the base material becomes so chemically reactive that the rate-limiting step to the reaction kinetics is diffusion of steam through a non-reactive gaseous boundary layer that forms at the surface of the base material. In the intermediate temperature range, Regime II, a transition occurs between the two rate limiting processes of Regimes I and III. Because dust layers are highly porous, the ability of steam to permeate into the dust layer, as the dust particles of this layer transition through these three oxidation regimes, will become a rate-limiting process at elevated dust layer temperatures and the point at which this permeation becomes a rate-limiting step will depend on the thickness of the dust. To model this process, the diffusion of steam into the dust layer and the counter diffusion of hydrogen out of the same layer, we adopted for our dust layer oxidation model the following steady state diffusion equation that describes the equimolar binary gaseous diffusion of Gas A ($H_2O$) into Gas B ($H_2$) when a chemical reaction occurs [5]:

$$-\mathbf{D}_{\mathbf{AB}}\frac{\mathbf{d}^2\mathbf{c}_{\mathbf{A}}}{\mathbf{d}^2\mathbf{z}}+\mathbf{R}=\mathbf{0} \qquad (1)$$

where

$D_{AB}$ is the binary diffusion coefficient of Gas A in Gas B ($m^2$/s)

$c_A$ is the molar concentration of Gas A (mole/$m^3$)

z is the distance perpendicular to the dust film surface (m)

R is the bulk reaction rate (mole-$H_2O$/$m^3$-s)

For the case of a porous film, the binary diffusion coefficient in Equation 1 should be replaced by an effective diffusion coefficient that accounts for the porosity of the layer and the tortuous diffusion path Gas A must make in order to permeate this layer, defined as follows:

$$\mathbf{D_{eff} = \tau \varepsilon D_{AB}} \quad (2)$$

where

$\tau$ is the tortuousity defined as the differential perpendicular distance of $z$ to that of the actual path length $s = (dz/ds)^2$

$\varepsilon$ is the porosity of the film

In theory, the bulk reaction rate of Equation 1 can be derived from the oxidation rates for fully dense beryllium, note Figure 1, if the effective surface area of dust particles in the layer is known. Fortunately, this area, $s_D$ the specific surface area density ($m^2/kg$), can be experimental measured by the BET gas absorption technique. Based on the specific surface area density the bulk reaction rate can be determined as follows:

$$\mathbf{R = s_D \rho_D R_{Be}^{INL} \kappa} \quad (3)$$

where

$s_D$ specific surface area density for the dust particle ($m^2/kg$)

$\rho_D$ dust density ($kg/m^3$)

$R_{Be}^{INL}$ INL beryllium-steam oxidation rate equation for fully dense beryllium ($kg\text{-}Be/m^2\text{-}s$)

$\kappa$ is a conversion factor from kg of Be to mole of $H_2O$ for this reaction

Figure 2 contains fully dense, 88% dense, pebble and dust oxidation information based on $s_D$ from References [4, 6, 7, 8]. As can be seen in this figure, the assumption that fully dense beryllium is as reactive as beryllium dust on a per unit area basis, e.g. the assumption behind Equation 3, is fairly accurate for Regime I, within a factor of two, but the transition to Regime II occurs at a much lower temperature for the fully dense beryllium than for the dust, making our oxidation model conservative.

The beryllium-steam oxidation rate is also dependent on the steam partial pressure. The fully dense beryllium oxidation equation of Figure 1 was developed at a steam pressure of 0.86 atm. Reference [9] suggests that

below 200 kPa this reaction will vary as steam pressure raised to 0.9 power ($p^{0.9}$). We approximate this behavior by assuming a first-order chemical reaction defined as:

$$\mathbf{R = k\,c_a} \tag{4}$$

where the reaction rate coefficient k is related to Equation 3 as follows:

$$\mathbf{k = \frac{s_D\,\rho_D\,R_{Be}^{INL}\,\kappa}{c_{H2O}}} \tag{5}$$

Here, $c_{H2O}$ is the molar concentration of the steam at the INL test conditions (27.7 mole/$m^3$).

With these definitions, Equation 1 becomes

$$\mathbf{-D_{eff}\frac{d^2c_A}{d^2z} + k\,c_A = 0} \tag{6}$$

Reference [10] gives the solution to this equation for boundary conditions of a defined concentration of $c_A^o$ at z equals zero and a non-flow boundary at z equals the layer thickness, δ (m), to obtain the steam concentration profile in the film as:

$$\mathbf{c_A = c_A^o\left[\cosh\left(\sqrt{k/D_{eff}}\;z\right) - \tanh\left(\sqrt{k/D_{eff}}\;\delta\right)\sinh\left(\sqrt{k/D_{eff}}\;z\right)\right]} \tag{7}$$

We can now derive a steam reaction rate based on the actual geometric surface area of the layer $R_s$ (kg-Be/$m^2$-s) by substituting Equation 7 into Equation 4, and integrating over the thickness of the layer. The resulting equation is:

$$\mathbf{R_s = \frac{k\,c_A^o}{\kappa\sqrt{k/D_{eff}}}\tanh\left(\sqrt{k/D_{eff}}\;\delta\right)} \tag{8}$$

Based on a recent communication, the dust layer density can be assumed to be 1.0 g/$cm^3$ [11]. At this density, the layer porosity is 0.45. If the dust particle diameter is set to the mass mean diameter for dust callout in SADL [9] of 2 μm, then all of the quantities necessary to allow a comparison between Equation 8 and the other beryllium-steam oxidation rate equations. This comparison also appears in Figure 2. Also included in the Figure 2 is a prediction from Equation 8 if the transition temperature between Regimes I and II is changed from 520°C to 700°C.

Because the beryllium-steam oxidation reaction is exothermic, the possibility exits for a thermal excursion to occur in a beryllium dust layer during the oxidation process. In order to accurately model this possibility, two

important heat transfer parameters were also developed for this dust layer model, those of an effective thermal conductivity for the beryllium dust and a contact conductance at the interface between the dust layer and other structures, such as the FW tiles or copper substrate. Heat conduction within the dust layer can occur by three predominate mechanisms: solid conduction within the dust particle plus thermal radiation between particles at the voids, conduction between particles by way of a gas that occupies the void, and contact conduction between adjacent dust particles. The equations used to determine the effective thermal conductivity for the dust layer are those present in References [12,13]. A more detailed description of this effective thermal conductivity model can be found in Reference [2].

Typically, heat transfer at such interfaces is modeled with a gap conductance heat transfer coefficient. It is assumed here that this approach is applicable to a dust-tile or dust-substrate interface. However, a correlation for dust gap conductance coefficients could not be found in the literature. As a consequence, a correlation for metal-to-metal gaps was used for our dust layer model. Heat conductance at such gaps is thought to be the sum of three contributions, that from metal contact, which is a function of contact pressure, plus that from interstitial gas conduction and thermal radiation in the gap [14]. For this model, the contact conduction term was ignored because of the lack of a mechanism that produces a mechanical load at this interface. As for the gas contribution, Reference [15] suggests that the gas contribution ($h_g$ W/m$^2$-K) can be estimated, based on the gas thermal conductivity ($k_g$ W/m-K), by the following equation:

$$\mathbf{h_g \approx \frac{k_g}{2.7\sigma}} \tag{9}$$

where $\sigma$ (m) represents the effective root mean square surface roughness at the gap defined as:

$$\sigma = \sqrt{\sigma_1^2 + \sigma_2^2} \tag{10}$$

where the subscripts (1, 2) refer to the two materials forming the gap. However, during operating conditions of a tokamak reactor, initially very little gas will be present in such gaps; and during accident conditions, this gas pressure could increase up to about 150 kPa before the ITER vacuum vessel (VV) pressure suppression system actuates and limits the VV pressure. In order to simulate this transition from vacuum to a collisional gas in this gap, the formula for effective gas conductivity in powder beds, cited in Reference [16], is used in Equation 9. This formula is as follows:

$$\mathbf{k_g^{eff} = \frac{k_g}{\frac{B}{p_g\sigma} + 1}} \tag{11}$$

where $p_g$ is the gas pressure (Pa). The coefficient B of Equation 11 is defined as

$$\mathbf{B} = \frac{\mathbf{4\gamma}}{\gamma + \mathbf{1}} \frac{\mathbf{2 - A}}{\mathbf{A}} \frac{\Lambda_o \mathbf{p_o}}{\mathbf{Pr}} \tag{12}$$

where

| | | |
|---|---|---|
| $\gamma$ | - | gas specific heat ratio |
| A | - | gas accommodation coefficient (taken as 1) |
| $\Lambda_o$ | - | molecular mean free path (m) of gas at pressure $p_o$ |
| $p_o$ | - | reference pressure (set at 100 kPa) |
| Pr | - | gas Prandlt number |

We have benchmarked this gap conductance model against data found in Reference [14] and found excellent agreement with tests that were conducted with a very low applied mechanical pressure, as demonstrated in Reference [2].

**3. Application of dust layer to an ITER wet bypass accident**

We have applied our model for analyzing a dust layer in ITER during a wet bypass accident. The postulated initiating event for this accident is an ex-vessel divertor primary heat transport system (PHTS) pipe break. A description of this accident can be found in the GSSR-Volume 7 [17]. We added our dust layer model to a MELCOR user input deck developed for the analysis of this accident. For this accident, it is postulated that during a plasma burn, a double-ended pipe rupture of the largest pipe occurs in the ex-vessel section of a divertor PHTS cooling loop. Coolant from this loop is discharged at a high rate into the heat transfer system (HTS) vault. The fusion power termination system will actuate on a high pressure signal from a pressure sensor in the vault or low water level sensor in the pressurizer of this primary cooling system, terminating the plasma burn by five seconds into this event. Even though the plasma burn is terminated, there is a possibility that the divertor cooling channels will undergo damage by melting prior to plasma termination. As a consequence, a bypass of the primary confinement barrier of ITER, which is the vacuum vessel, occurs as a result of this accident. Of primary safety concern during this accident regarding this dust layer modeling effort is whether or not the beryllium dust on the FW will undergo significant oxidation during such events, producing unsafe levels of hydrogen from the beryllium-steam oxidation reaction.

In order to perform this analysis, we had to make two additional assumptions. The first assumption was that all of the dust resides in the grooves between FW beryllium titles. The quantity of beryllium dust estimated to

reside in the ITER VV as a result of erosion of the FW by plasma particle impact is 100 kg [9]. If this dust resides in these groves, the dust layer would have a surface are of ~37 $m^2$ and a thickness of ~2.8 mm. The second assumption is that the dust layer experiences the same surface heating as the rest of the FW, an assumption that conservatively ignores the shadowing effect of the thicker FW beryllium tile (10 mm thick).

Our first set of analyses were designed to parametrically determine how low the gap conductance at the tile and substrate interfaces would need to be for the dust layer to undergo a significant thermal excursion, resulting in the majority of the dust oxidizing. Figure 3 contains the predicted dust layer surface temperature for gap conductance heat transfer coefficients of 500 W/$m^2$-K, 250 W/$m^2$-K, and 100 W/$m^2$-K. As can be seen, thermal runaway occurs for a gap coefficient of 100 W/$m^2$-K. There are two temperature histories for a gap coefficient of 100 W/$m^2$-K. The first history is for a case where beryllium evaporation is allowed to occur. This evaporation carries heat away from the surface, and thereby limits the surface temperature. For this case, the dust oxidation terminates as result of a complete oxidation of the dust layer. The second history is for a case that assumes that the beryllium dust oxidation process results in a portion of the beryllium layer turning into beryllium oxide (BeO), and at high dust layer temperatures this BeO layer will form primarily at the layer surface. As a result, this surface oxidation will produce a growing beryllium oxide film through which steam must diffuse before it can react with the beryllium beneath the developing oxide film. For this case, 80% of the dust layer oxidizes before the produced oxidation energy falls below that energy lost by heat conduction to the Be tiles and Cu substrate.

Given these results, we reran the wet bypass accident scenario allowing the dust layer gap conductance model (Equ. 11) to predict the gap coefficient. The resulting dust layer surface temperature is shown in Figure 4. As can be seen in this figure, initial the dust layer temperature is quite high (~1400 K) because the only mode of heat transfer at the gap is radiation heat transfer. However, soon after the steam enters the VV by way of the in-vessel divertor break, the enhanced gap conductance produced by steam and/or hydrogen gas conductivity provides a cooling rate by way of the FW tiles and substrate that is greater than the heat produced by the chemical oxidation of the dust layer. The result is a rapid drop in dust layer temperature, as opposed to a thermal runaway, and only 25% of the dust layer oxidizing. The predicted dust layer gap conductance heat transfer coefficient during this accident is given in Figure 5. While these results are encouraging from a safety

standpoint, further experimental research into dust oxidation and heat transfer is required to validate these results.

**4. Summary**

In this paper we have presented the theoretical basis for a beryllium dust oxidation model that has been developed at the INL for the MELCOR safety computer code. The purpose of this model is to predict hydrogen production from steam reactions in beryllium dust layers on hot surfaces inside a fusion reactor VV during in-vessel LOCA. In addition, a second goal of this modeling effort was to develop a flexible capability that allows the user to investigate different dust layer depths, and heat transfer boundary conditions. To accomplish this, a beryllium dust oxidation model was developed that accounts for the diffusion of steam into a beryllium dust layer, the oxidation of the dust particles inside this layer based on the beryllium-steam oxidation equations developed at the INL, and the effective thermal conductivity of this beryllium dust layer.

We have applied this oxidation model to a wet bypass accident scenario in the ITER device. The results indicate that even with our conservative oxidation model that a thermal runaway of the dust layer, due to the chemical heat produced by the beryllium-steam reaction, does not occur. Our model also predicts that due to the high initial dust layer temperature, resulting from a conservative assumption of dust layer surface heating by the plasma, less than 1% of the 100 kg of beryllium dust will oxidize before the dust layer temperature returns to temperatures where very little additional oxidation is anticipated. However, further experimental research into dust oxidation and heat transfer is required to validate these results.

**Acknowledgement**

This work was prepared under the auspices of the US Department of Energy, Office of Fusion Energy Science, under the DOE Idaho Field Office contract number DE-AC07-05ID14517.

**References**


1 Gauntt et al., MELCOR computer code manuals, NUREG/CR-6119 , SAND2000-2417/2 , Vol. 2 , Rev 2 , version 1.8.5 , October 2000.

2 ITER Implementing Task Agreement (ITA), "Support and assistance for the latest fusion versions of computer codes," ITA 81-08, extension G 81 TD 21 FU, January (2005).

3 M. Rossberg, E. Wicke, "Transportvorgänge und Oberflä-chenreaktionen bei der Verbrennung graphitischen Kohlenstoffs," *Chemie-Ingenieur-Technik*, 3, (1956) 181-189.

4 K. A. McCarthy, et al., "The Safety Implications of Tokamak Dust Size and Surface Area," Fusion Engineering and Design, 42, 1998, p. 45-52.

5 J. R. Welty, C. E. Wilson, and R. E. Wilson, *Fundamentals of Momentum, Heat and Mass Transfer*, John Wiley & Sons, Inc., New York, 1969, p 495.

6 G. Smolik et al., "Reaction of porous Beryllium in Steam", INEEL, EGG-FSP-10346, July 1992.

7 R. A. Anderl, R. J. Pawelko, "Steam Chemical Reactivity of Beryllium Powder," INEEL/EXT-99-00338, April 30, 1999.

8 D.A. Davydov, B.N. Kolbasov, "Dust in Cavity Reactivity Measurements," ITER Russian Home Team Final Report on task agreement G 81 TT 09 FR, Bochvar All-Russian Scientific Research Institute for Inorganic Materials (VNIINM) Report: RF 01 VNIINM SHE-1, July, 2001.

9 ITER, "Safety Analysis Data List," G 81 RI 10 03-08-08 W 0.1, Version: 4.0.3 SADL, September 26, (2003)

10 F. P. Incropera, and D. P. DeWitt, *Fundamentals of Heat and Mass Transfer (3rd Edition)*, John Wiley & Sons, Inc., New York, 1981, p. 903.

11 Private communication by email with ITER IT ITA task officer Leonid Topilski, July 26, 2005.

12 P. Zehner, and E. U. Schlünder, "Thermal Conductivity of Granular Material at Moderate Temperatures," *Chemie-Ingr-Tech*, 42, pp933-941, 1970. In German.

13 G. Breitbach, and H. Barthels, "The Radiant Heat Transfer in the HTR Core After Failure of the Afterheat Removal Systems," *Nuclear Technology*, 49, pp392-399, August 1980.

14 S. Song, M. M. Yovanovich, and K. Nho, "Thermal Gap Conductance: Effects of Gas Pressure and Mechanical Load," *Journal of Thermophysics and Heat Transfer*, Vol. 6, No 1, (1992), p. 62-68.

15 W. Cheng, and C. Madhusudana, "Decrease in Thermal Contact Conductance and the Contact Pressure of Finned-Tube Heat Exchangers Assembled with Different Size Bullets," *Journal of Heat Transfer*, 129, July (2007), p. 907-911.

16 M. Shapiro, et al., "Characterization of Powder Beds by Thermal Conductivity: Effect of Gas Pressure on the Thermal Resistance of Particle Contact Points," *Particle & Particle Systems Characterization*, 21 (2004), p. 268-275.

17 ITER Technical Basis, "Plant Description Document," International Atomic Energy Agency Document, G A0 FDR 1 01-07-13 R1.0, January (2002), p. 5-45.

**Figure 1.** INL beryllium-steam oxidation rate equations for fully dense beryllium indicating three distinct oxidation regimes.

**Figure 2.** Comparison of beryllium-steam oxidation rate equations based on measured specific surface area densities compared with Equation 8 of this article.

**Figure 3.** Dust surface temperature during a wet bypass accident for different dust to tile gap conductances.

**Figure 4.** Dust surface temperature during a wet bypass accident when Equation 9 is used to predict dust to tile gap conductance.

**Figure 5.** Dust to tile gap conductance during a wet bypass accident when Equation 9 is used to predict gap conductance.

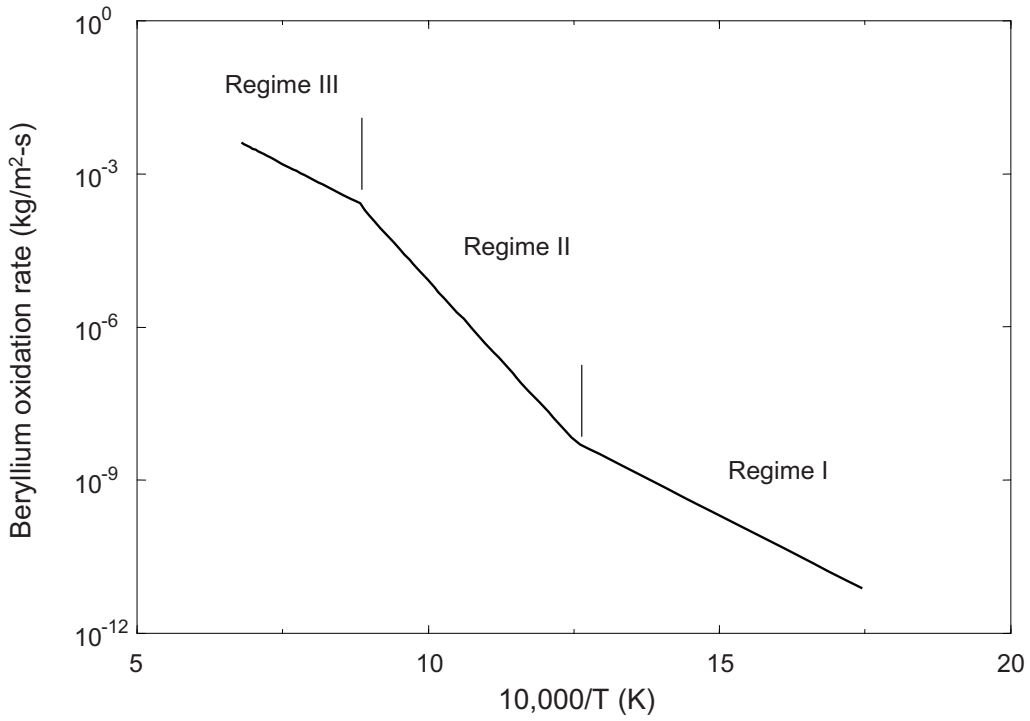
Regime III
Regime II
Regime I
Beryllium oxidation rate (kg/m2-s)
10,000/T (K)
10^0
10^-3
10^-6
10^-9
10^-12
5
10
15
20

**Figure 1.**

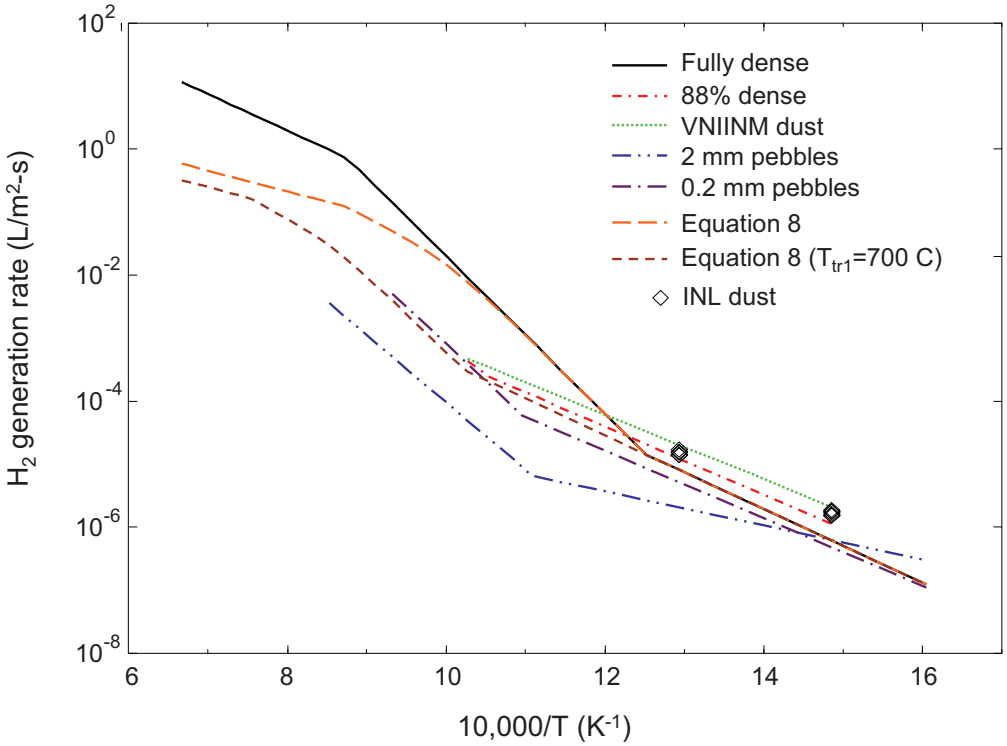
Fully dense
88% dense
VNIINM dust
2 mm pebbles
0.2 mm pebbles
Equation 8
Equation 8 (T$_{tr1}$=700 C)
INL dust
H$_2$ generation rate (L/m$^2$-s)
10,000/T (K$^{-1}$)
10$^2$
10$^0$
10$^{-2}$
10$^{-4}$
10$^{-6}$
10$^{-8}$
6
8
10
12
14
16

**Figure 2.**

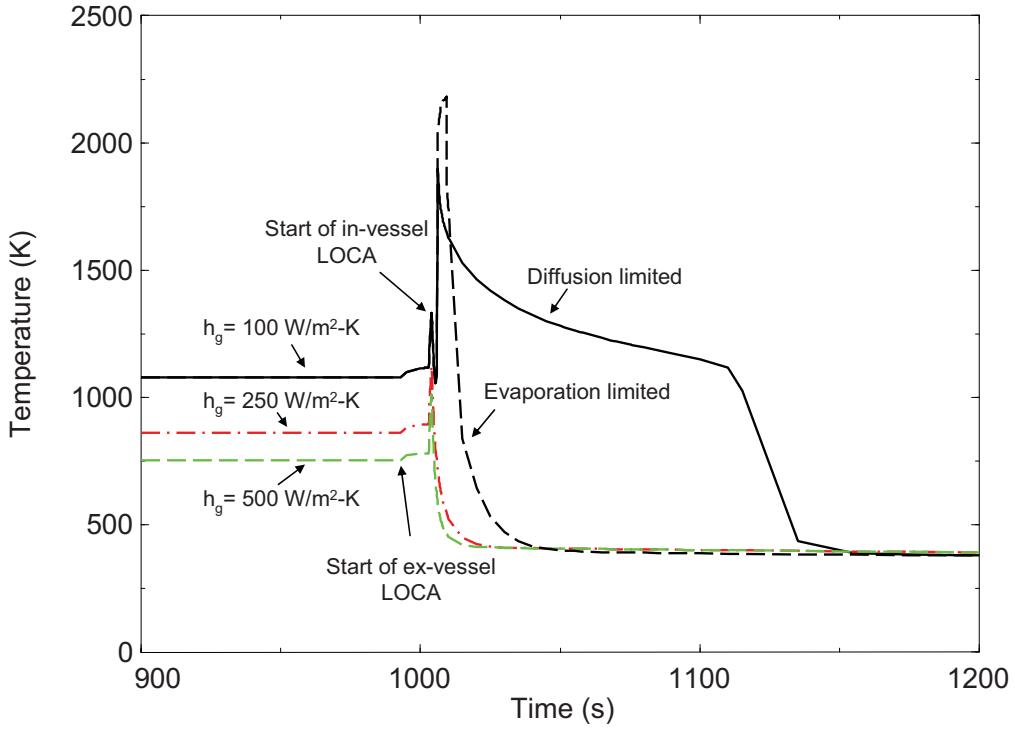
2500
2000
1500
1000
500
0
Temperature (K)
900
1000
1100
1200
Time (s)
Start of in-vessel
LOCA
Diffusion limited
h_g= 100 W/m²-K
h_g= 250 W/m²-K
Evaporation limited
h_g= 500 W/m²-K
Start of ex-vessel
LOCA

**Figure 3.**

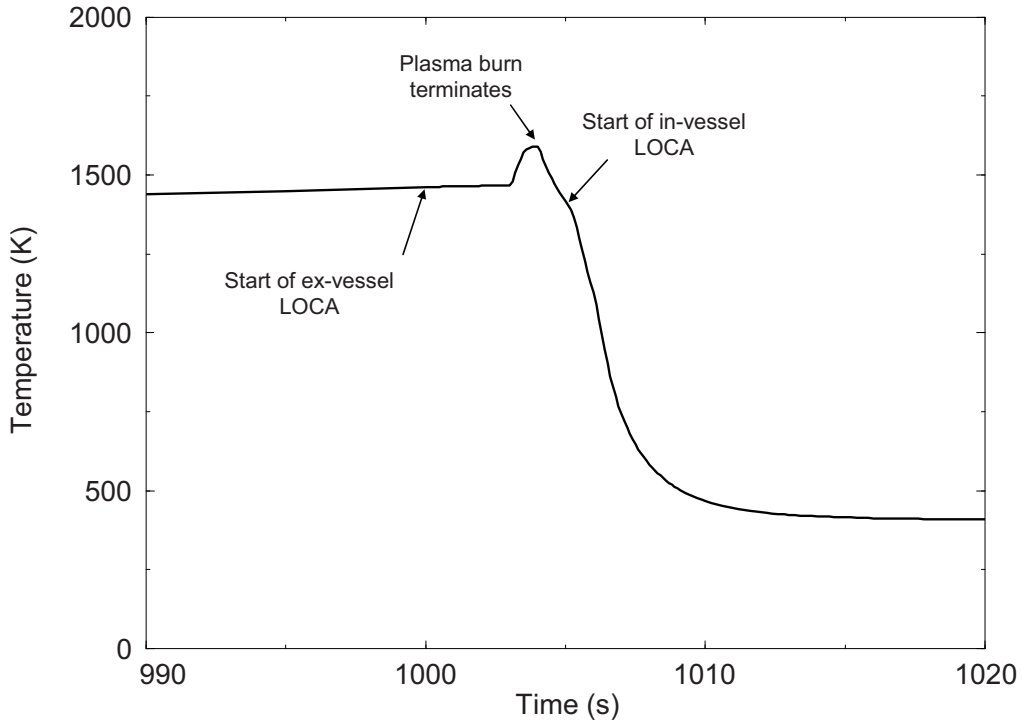
2000
1500
1000
500
0
Temperature (K)
990
1000
1010
1020
Time (s)
Plasma burn
terminates
Start of in-vessel
LOCA
Start of ex-vessel
LOCA

**Figure 4.**

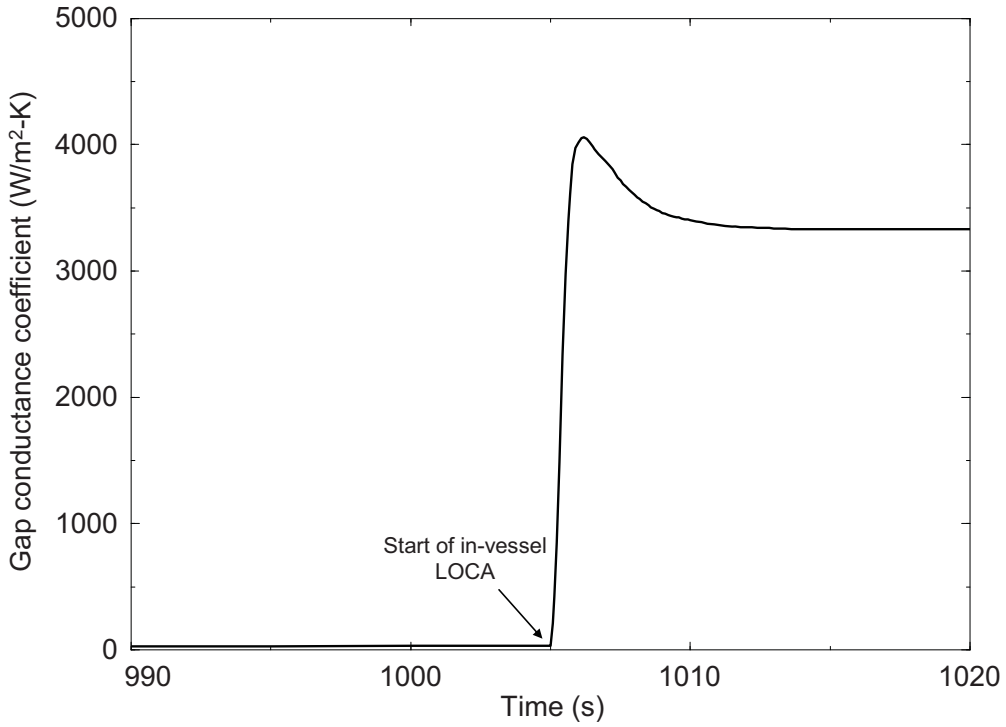
5000
4000
3000
2000
1000
0
Gap conductance coefficient (W/m2-K)
Start of in-vessel
LOCA
990
1000
1010
1020
Time (s)

**Figure 5.**